IEEE Access
Multidisciplinary | Rapid Review | Open Access Journal

Date of publication xxxx 00, 0000, date of current version xxxx 00, 0000.

Digital Object Identifier 10.1109/ACCESS.2022.0092316

Research on coal volume detection and energy-saving optimization intelligent control method of belt conveyor based on laser and binocular visual fusion

LIANG WEN[1,2], BING LIANG[1], LIYA ZHANG[2],(MEMBER, IEEE), BONAN HAO[2], ZHIFANG YANG[2]

[1]School of mining, Liaoning Technical University, Fuxin 123000,China
[2]CCTEG China Coal Research Institute, Beijing 100013,China

Corresponding author: Liang Wen (e-mail: 1448632527@qq.com).

This work was supported in part by the Science and Technology Innovation and Entrepreneurial Fund Special Project of CCTEG Tiandi Science Technology Co., Ltd.(2022-TD-ZD001), in part by the Science and Technology Development Fund Project of CCTEG China Coal Research Institute (2022CX-I-06, 2021CX-II-16)

ABSTRACT

Real-time coal flow monitoring is crucial for efficient coal mine transportation. Traditional vision acquisition devices generate two-dimensional images that are not accurately identified in the complex underground coal mine environment, such as dust, water mist, and low light. In this paper, we propose a conveyor belt coal flow detection method that integrates laser scanning and binocular vision to address this problem. Our proposed method has several advantages over traditional approaches. Firstly, we calibrate the binocular camera using Zhang's calibration method to enhance the accuracy of the system. Secondly, we extract the centerline of the laser stripe using the grayscale center of gravity method, which improves the system's performance in complex environments. Thirdly, we calculate the cross-sectional area of the material accurately using the trapezoidal area accumulation method, and visualize it in two dimensions based on a single frame, while the point cloud data from multiple consecutive frames are visualized in a 3D model at a realistic scale. Finally, we use the continuous multi-frame cross-sectional area to calculate the current conveyor flow, and apply the BP neural network to establish an energy-saving optimization model for the belt conveyor. We also design a PLC fuzzy controller based on fuzzy control algorithms to adjust the belt's operating speed intelligently according to the coal flow size, achieving energy-saving operation and intelligent control of the belt conveyor. Our experiments show that our method can accurately obtain coal volume and control the belt speed of the conveyor in real-time, making it an innovative and practical solution for coal flow detection and energy-saving operation in underground coal mines.

INDEX TERMS machine vision; stereo matching; energy-saving optimization; coal volume detection; belt conveyor

I. INTRODUCTION

IN the process of mechanized transportation of coal, due to the unevenness of coal mining, the conveyor often belongs to the air-loading rapid operation status. Therefore, the speed adjustment of the air-loading conveyor according to the coal volume is urgent to solve. However, the manual control method is still the main method of controlling traditional conveyor control. And due to the complex environment of the underground, the coal dust has a greater impact on the sight of the workers, which makes the equipment control error greater. Therefore, the real-time automation and precise coal volume measurement is the key to realizing the speed control of the belt conveyor, the energy conservation, consumption reduction and intelligent mining.

The current method for the detection of conveyor coal volume mainly includes electronic belt scale [1], nuclear scale, ultrasonic detection [2], laser instrument detection [3], visual detection and etc. There are many limitations for the

application of electronic belt scale and nuclear term [4]; The accuracy of ultrasonic detection in a complex coal mine production environment is difficult to guarantee. In recent years, laser detection [5], machine visual detection and other non-contact methods are widely used due to high accuracy and low environmental impact. Yuan Wang [6] proposed PDS-Algorithm (Planar Density Simplification Algorithm) used in the detection of abnormal coal flow of a coal mine scraper conveyor and the results show that the proposed abnormal flow monitoring method can meet the accuracy and real-time requirements of coal mine abnormal alarms. Guimei Wang [7] presented a method of coal volume detection and classification based on machine vision and deep learning. Yongqing Lv [8] designed a dynamic measurement system of coal volume on belt conveyor based on image processing, which can automatically adjust the speed of multiple belt conveyors.

During the operation of the belt conveyor, the operating resistance is needed during operation. Operating resistance is the main cause of mechanical loss and cannot be eliminated. Too much resistance to the belt conveyor will not only cause energy loss, but also accelerate the wear of the equipment and shorten its service life. Hiltermann [9] provided a methodology to predict these savings with the use of DIN 22101. Shirong Zhang and others [10] intended to take a model based optimization approach to improve the efficiency of belt conveyors at the operational level. Jianhua Ji [11] proposed a power consumption model of the belt conveyor system, and a energy-saving control strategy of the belt conveyor with variable belt speed based on the material flow rate was put forward.

In summary, there are relatively few studies that integrate multiple non-contact measurement methods. Therefore, we proposed a detection method by fusing laser and binocular vision information to achieve the measurement of the conveyor belt coal volume and we achieved the goal to combine high direction ability of the laser with the high-precision characteristics of the binocular vision. For more clarity, the main contributions of this work are summarized as follows:

(1) A merging laser scanning and binocular visual coal flow detection method was proposed, which can greatly reduce the impact of measurement accuracy in coal mines and the harsh environment at the first attempt.
(2) The binocular visual camera calibration system was studied and the image filtering and cutting were pre-processed using image filtering and cutting, reducing the actual computing amount and improving the real-time nature of the system.
(3) The energy-saving operation and intelligent control of the belt conveyor was achieved by using BP neural network and PLC fuzzy controller, which achieved that the operating speed of the belt can be intelligently adjusted according to the size of the coal flow volume.

II. OVERALL DESIGN

The process of the coal detection system based on laser and binocular visual fusion is shown in Figure 1. The idea of the overall design for the detection method is to fuse the line laser and the binocular vision information. The line laser and the binocular camera are fixed to the front of the conveyor band through a bracket. The line laser is projected on the contour of the coal material on the conveyor belt by direct radiation. The height difference between the point cloud during the air-loading and the runtime is accumulated to the current volume flow and the coal flow is calculated based on the accumulation density constant of the coal.

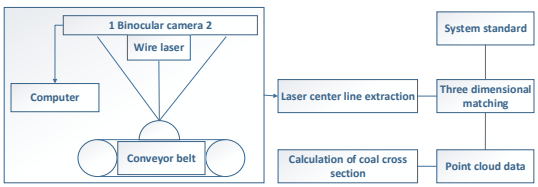

FIGURE 1. System overall process

The system is mainly composed of strip conveyor, line laser transmitter, binocular vision stereo camera, camera fixed rack, computer and other equipment. Sink belt conveyor: It has a large loading capacity, transportation capacity and it can simulate the material transfer through the slot conveyor as the basis of the volume detection system; Line laser transmitter: It can perform low power consumption and high efficiency power output, strong direction, high brightness, high recognition and stable performance; Strong anti-interference is suitable for harsh working environments. Collecting images mainly processes projected laser stripes to obtain precise contour information on the surface of material projection. Three-dimensional binocular camera [12], [13] is similar to human eyes, the visual information that can be obtained by the same object. It is the basis for the visual measurement of the machine. The frame rate and image quality collected by the binocular camera determine the calculation complexity and results accuracy.

III. THREE-DIMENSIONAL BINOCULAR CAMERA CALIBRATION AND CORRECTION

The essence of three-dimensional calibration is to establish the corresponding relationship between camera image pixels and actual space point location information. Therefore, the mathematical equation between the physical space coordinate system and the image coordinate system can be calculated as follows:

$$Z_c \begin{bmatrix} u \\ v \\ 1 \end{bmatrix} = \begin{bmatrix} \frac{f}{d_x} & 0 & u_0 & 0 \\ 0 & \frac{f}{d_y} & v_x & 0 \\ 0 & 0 & 1 & 0 \end{bmatrix} \begin{bmatrix} R & T \\ 0^T & 1 \end{bmatrix} \begin{bmatrix} X_w \\ Y_w \\ Z_w \\ 1 \end{bmatrix} = M_1 M_2 X \tag{1}$$

where X is the point coordinate in the physical space; Z_c is the coordinate conversion coefficient; M_1, M_2 is the internal and external parameters of the camera; f is the

focal length; d_x, d_y are the high and width of single pixel, respectively; u_0 is the horizontal coordinate value; v_0 is the vertical coordinate value. T, R are the translation matrix and rotating matrix, respectively.

We applied Zhang's calibration method [14]. The use of a plane checkerboard grid for calibration, compared with the photography calibration method, overcomes the disadvantages of three-dimensional standards that require high precision; compared with the self-standard method, the problem of poor robustness of the self-calibration method is solved. The calibration process only needs to shoot multiple groups from different angles.

We must calibrate the left and right cameras alone and consider the overall calibration. So we use the rotating matrix R and the displacement matrix T to describe the corresponding relationship of the left and right camera pixel coordinate system, which can be calculated as follows:

$$p_l = Rp_r + T \tag{2}$$

The rotating matrix and the displacement matrix of the left and right cameras are represented by R_l, R_r, T_l, T_r, separately, which means that the overall calibration of R and T matrix can be represented as follows:

$$\begin{cases} R = R_l R_r^{-1} \\ T = T_l - RT_r \end{cases} \tag{3}$$

IV. LASER SPOT IMAGE PROCESSING

A. LINE LASER STRIPE CENTER LINE EXTRACTION

After installing the line laser and the binocular camera, make sure that the laser stripes projection and the public vision are in both public vision and manual adjustment makes the laser stripes vertically with the binocular connection. When the system is working, we obtain the laser stripe images from the left and right cameras. And then, the images will be cut and the laser stripes are retained to ensure they can still be kept within the public vision range of the binocular visual camera with the material. Extracting the central line of laser stripes, the accuracy of this step will directly affect the error of the point cloud data, which is also the key to the final calculation of the coal volume. When the belt conveyor is empty, the central line obtained by the laser spots can be used as the benchmark line on the surface height of the conveyor belt.

1) line laser stripe feature analysis

The system selects a line laser light source. The intensity distribution of the laser transmitter stripes in the width is similar to the Gaussian function, which can be calculated as follows:

$$G(x) = A \times \frac{1}{\sigma\sqrt{2\pi}} \times \exp\left[-\frac{(x-u)^2}{2\sigma^2}\right] \tag{4}$$

During the actual laser project, due to various external factors, the laser wiring will be disturbed by some noise, damaging the quality of the image and generating irregular discrete data points. Common noise includes the noise of the camera, mechanical vibration noise and external environmental noise. Because these external factors cannot be completely avoided, the images are preprocessed to remove interference that is not conducive to the central line extraction.

2) Laser image preprocessing

The main function of the image preprocessing is to gray the collected laser stripe signals and perform smooth noise reduction processing. Laser stripe components are single. The light strip area and dark background area are compared with obvious comparison, so we use a spatial filtering method. Space filtering method includes mean filtering, medium value filtering and bilateral filtering. Compared with two other filtering methods, the average filtering uses a linear filtering method, which will only blur the edge of the image. The image information is less than the granular noise in the image obtained by scanning. Select the average filtering method to smooth the line laser stripes. The laser stripes and grayscale images before and after filtering are shown in Figure 2 and 3. After smooth filtering, the laser stripes become smooth and continuous in the width direction and the noise of the laser stripe edge is effectively filtered.

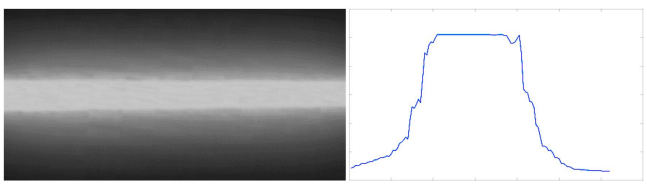

FIGURE 2. Before filtering laser stripes and grayscale images

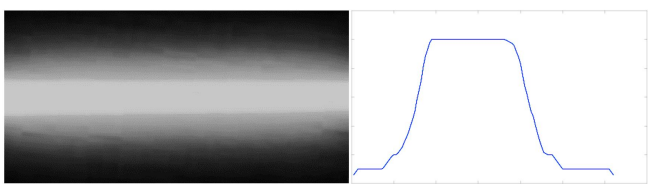

FIGURE 3. Laser stripes and grayscale images after filtering

3) Laser stripe center line extraction

Line laser transmitter has the characteristics of good direction and aggregation, line laser irradiation still has a certain width when a light is on the surface of the object. The laser stripes on the image are not a single-pixel width line. It is not suitable for subsequent calculations. Therefore, a specific point needs to be selected. Therefore, we should choose a specific point as the center point of the laser stripe, so as to determine the center line of the line pixel width. The extraction method for the center line of the line laser stripes includes the geometric center method and the energy center method.

The geometric center methods include the edge center extraction method and morphological skeleton extraction method:

- Edge Center Extraction Method [15]: The edge method is based on one edge as a light stripe center. The center method is to extract the inner edge of the inner edge of the light stripes on the basis of the edge method as the centerline of the light stripes. It is required that the quality of the image is high and the structural light characteristics are high. Because the shape of the coal is not regular, it has a greater impact on the extract of the structural optical bars.
- Morphological skeleton extraction method: The laser stripes are continuously corrosive, until the single pixel level laser stripes are connected. Because the refinement method is based on morphological methods and does not consider the characteristics of the cross-section gray distribution of light stripes, the central line accuracy of refined and extracted is still limited.

The energy center methods [16] include energy center law extreme value method, threshold method and gray gravity method:

- Energy Center Law Extreme Value Method: The gray degree distribution function of the cross section of the light strip is required, and the gradient operation is required. The gradient value is zero, which is the current section stripe center. Although this method is fast, the grayscale distribution of stripes can not form a Gaussian distribution curve with approximate ideal, so it is difficult to use the image with less signal noise.
- Threshold Method: Select a grayscale value according to the strong distribution of laser light as a threshold K, and find the left and right boundaries corresponding to the laser stripes corresponding to the K value. The threshold method is fast, the algorithm is simple, but it is easy to be affected by noise, and the extraction accuracy is poor.
- Gray Gravity Method: This method has been improved on the basis of the extreme value method and threshold method. For laser wiring with uneven brightness, the quality heart in the gray value distribution is used as the center of laser stripes. Each gravity threshold for the extract of the line laser image matrix is different, which makes up for the lack of extraction of the fixed threshold method, reducing the problem of the line laser stripes caused by the uneven distribution of light and increasing the accuracy of the extract of the line laser center point.

Based on the above considerations, the gray gravity method in the energy center law is selected for experiments. The extract of the line laser stripe center line is shown in Figure 4. The result of the striped center line extracted by the gray gravity method is accurate and the curve is smooth. It proves that this method can overcome some noise interference and is in line with the actual laser lines projected on an object.

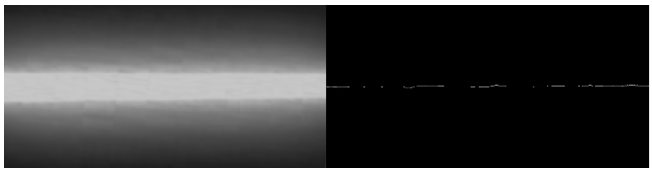

FIGURE 4. Line laser stripe center line extraction result

B. CORRESPONDING POINT OF THE IMAGE CORRESPONDING TO THE THREE-DIMENSIONAL MATCHING

After the laser stripe center line is processed, combined with the binocular camera calibration parameters, the left and right images are combined with three-dimensional matching [17], [18] to find the corresponding relationship in the two images. Due to the special placement of the camera and the laser, the central line of the laser stripes in the left and right cameras is the matching object. From the principle of geometry and unique constraints of the polar wire, the corresponding laser stripe center point in the left and right images is the corresponding matching point of each other. The principle of three-dimensional matching is shown in Figure 5. It is easy to calculate the visual distance after finding the corresponding matching point of the left and right images and then we can estimate the spatial position of the pixel point based on the relationship between the vision and distance. The three-dimensional matching algorithm is mainly local matching, global matching and semi-global matching.

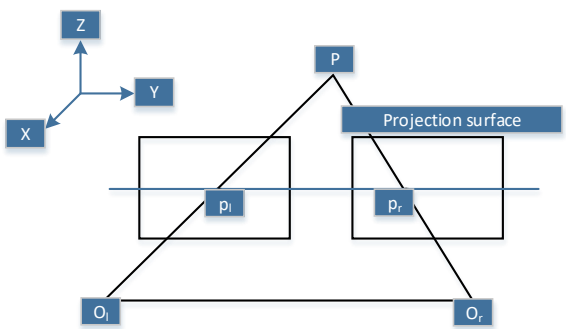

FIGURE 5. The principle of three-dimensional matching

- Local Matching: Select a small window, extract the characteristic vector of the image in the window, use the extracted feature vector to traverse the images that have not been matched and calculate the feature vector and traversal window extraction of the window during the traversing search process. The degree of the characteristics of the characteristic vector, the final result of the matching is the window with the largest degree of the characteristics of the characteristic vector. Matching accuracy is greatly affected by the window size.

- Global Matching: By processing the global dialogue information of the image, the global or local minimum value is found using the global energy function. This method matches high accuracy, but the algorithm is running for a long time and poor real-time. It is not advisable to be a three-dimensional matching algorithm for the coal detection system.
- Semi-global Matching: Select the visual difference for each pixel point to form an initial vision diagram, and then set a global energy function, which is related to the visual diagram. The best visual difference of pixels. Compared with the above two matching algorithms, it is faster than the local matching algorithm, and the region is larger. Compared with the global matching algorithm, it has not achieved global optimization considerations and improves real-time processing.

In summary, the semi-global matching algorithm is selected to deal with the image of the binocular images.

C. DIANYUN DATA ACQUISITION

After finding the matching point through the semi-global three-dimensional matching point, based on the principle of visualization of visual technology and the principle of polar line constraints, the two-dimensional to three-dimensional conversion is completed, and the three-dimensional coordinates of the corresponding point of laser stripes are calculated. The calculating formula is shown as follows:

$$X_l = \frac{T_x\,(x - \widehat{c}_{xl})}{D} Y_l = \frac{T_x\,(y - \hat{c}_{yl})}{D} Z_l = \frac{T_x f_x}{D} \tag{5}$$

where X_l, Y_l, Z_l are the three-dimensional coordinates for the center point of laser stripes compared to the left camera; x, y are the two-dimensional coordinates for the center point of the laser stripes on the left camera imaging; T_x is the‘ translation vector in the X-axis direction; The left camera coordinate for the three-dimensional correction of the two-dimensional camera; The focal length of the camera X axis. $\widehat{c}_{xl}, \hat{c}_{yl}$ are the left camera photoelectric coordinate after the three-dimensional correction of the two-dimensional camera; f_x is the focal length of the camera X axis. The left and right images are constantly calculated during the test. Each frame is continuously calculated to obtain the contour-point cloud data on the current material stack and the surface information is collected as the surface depth of the conveyor belt when the teleport is empty.

V. COAL VOLUME CALCULATION

After obtaining each frame of laser stripes point cloud data, the depth information on the surface of the conveyor belt is performed. The laser-striped point cloud data obtained when the teleportation belt is contained in the material surface is regarded as the outline information on the surface of the material. The flow on the belt conveyor refers to the quality of the transportation coal volume on the conveyor belt within the unit of time. The calculation method is the volume of the coal material on the entire conveyor belt in the unit time T. Calculating formula is shown as follows:

$$Q(t) = \rho V(t) \tag{6}$$

where $Q(t)$ represented the coal flow, ρ means the average density of coal, and $V(t)$ indicates the coal volume of the coal of entire conveyor belt within the unit of time. For the extraction center line of the surface line of the coal material, connect the two adjacent laser spots, and the two adjacent points can be regarded as trapezoids in the vertical direction. The sum of the trapezoidal area. The accumulation method of trapezoidal area is shown in Figure 6.

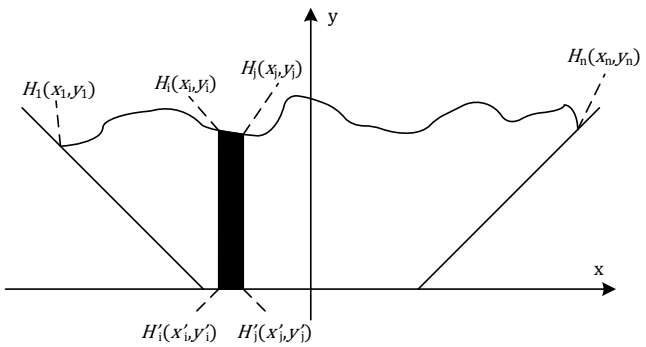

FIGURE 6. Capacity method of trapezoidal area

The starting point of the horizontal cross-section for the coal is the leftmost point$H_1(x_1, y_1)(n > 1)$ and the termination point is the right side $H_n(x_n, y_n)(n > 1)$. We selected the groove conveyor belt as a belt conveyor for coal transportation production. The roller on the left and right sides is up and up to form a groove with the horizontal roller. According to the laser contour point on the surface of the coal material, the point cloud data is divided one by one along the vertical direction of the X-axis, and the trapezoidal area between every two points is calculated, that is the closed area of $H_i(x_i, y_i), H_j(x_j, y_j), H_i'(x_i', y_i'), H_j'(x_j', y_j')$, in Figure 6. It is the surface data point measured by the conveyor belt when the belt conveyor is empty. According to the laser scanning condition, the surface contour of the transmitted belt surface contours of the laser point cloud data $H_i'(x_i', y_i')...H_j'(x_j', y_j')$, of the teleportation belt is extracted.

$$S_i = \frac{1}{2}\left[(y_i - y_i') + (y_j - y_j')\right]|(x_j - x_i)| \quad (1 \leqslant \mathrm{i} \leqslant \mathrm{n}, 1 \leqslant \mathrm{j} \leqslant \mathrm{n}) \tag{7}$$

As a result, the laser contour can be divided into $n-1$ adjacent trapezoids and the total section area is calculated:

$$S = \frac{1}{2}\sum_{i=1}^{n-1}\left\{\left[(y_i - y_i') + (y_{(i+1)} - y_{(i+1)}')\right] \times \left|(x_{(i+1)} - x_i)\right|\right\} \tag{8}$$

Suppose the frame rate f of the three-dimensional camera, the speed $v(t)$ of the conveyor belt, and the current instantaneous cross-sectional area obtained by the calculation is $S(i)$.

Then the coal flow volume of the teleportation belt within the unit time is $\frac{1}{f}$ time volume, set k the number of sections in the coal material in the unit time t and the average density of the coal material is ρ. Based on the above, the calculation formula of the coal flow of the system within the unit of time is:

$$\mathrm{Q(t)} = \rho \sum_{\mathrm{i=1}}^{\mathrm{k}} \frac{1}{\mathrm{f}} \mathrm{v(t)S(i)} \tag{9}$$

VI. CONSTRUCTION OF ENERGY-SAVING OPTIMIZATION MODEL AND DESIGN OF FUZZY CONTROLLER FOR BELT CONVEYOR

A. CONSTRUCTION OF ENERGY-SAVING OPTIMIZATION MODEL

The energy-saving optimization model of the belt conveyor is designed with a three-layer BP neural network structure, as shown in Figure 7. There are 2 nodes in the input layer: the coal flow volume Q and the belt running speed v of the belt conveyor; the output layer has 1 node: the power of the belt conveyor; Middle layer can be adjusted repeatedly according to the training situation until it meets the training requirements. IW_1 represents the hidden layer rights matrix, B_1 represents the deviation matrix of the hidden layer, IW_2 represents the power matrix of the output layer, and B_2 represents the deviation matrix of the output layer. In addition, the hidden layer activation function uses the Sigmoid function, and the output layer activation function uses a linear function.

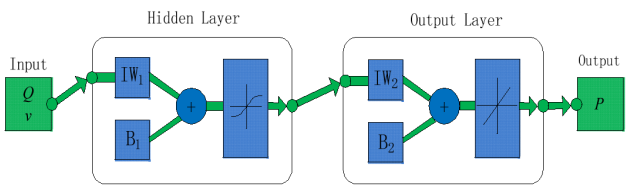

FIGURE 7. Structure of energy-saving optimization model

B. DESIGN OF FUZZY CONTROLLER

The fuzzy control theory is introduced to the belt conveyor based on the PLC as the control core. The belt speed v_0 is determined based on the coal flow rate obtained from the electronic belt scale, the actual belt speed v is obtained from the speed sensor, the deviation e and the rate of change in deviation ec are used as inputs to the fuzzy controller, and the frequency signal f is set by the frequency converter is used as the output of the fuzzy controller, thus establishing a PLC-based two-input, one-output fuzzy controller. The fuzzy language for e, ec and f are E, EC and F, respectively.

In the belt conveyor fuzzy controller, the basic domain of e is $[-e, e]$, the basic domain of ec is $[-ec, ec]$ and the basic domain of f is $[-f, f]$. The variables need to be converted from the fundamental domain to the modal domain. The quantified domains of the input variables E and EC are $\{-6, -5, -4, -3, -2, -1, 0, 1, 2, 3, 4, 5, 6\}$. the corresponding subset is $\{NB, NM, NS, Z, PS, PM, PB\}$,

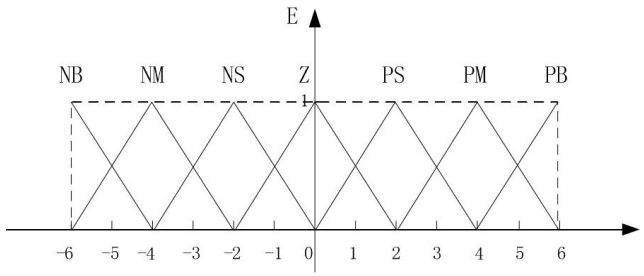

FIGURE 8. Membership function of E

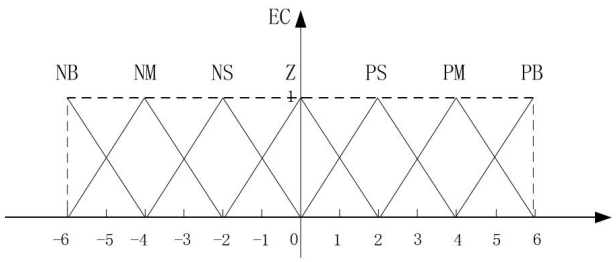

FIGURE 9. Membership function of EC

all using the triangle function as the affiliation function. The output variables F are all quantified in the domain of $\{-6, -5, -4, -3, -2, -1, 0, 1, 2, 3, 4, 5, 6\}$ and the corresponding subsets are $\{NB, NM, NS, Z, PS, PM, PB\}$, and the triangle function is chosen as the affiliation function. Figure 8 shows the affiliation function of input variable E, Figure 9 shows the affiliation function of input variable EC, and Figure 10 shows the affiliation function of output variable F.

Once the fundamental and fuzzy domains of the input and output variables have been determined, the corresponding quantization factors k_e, k_{ec}, k_f and scaling factor k_f can be calculated as follows:

$$\begin{cases} k_e = \frac{n_1}{e} \\ k_{ec} = \frac{n_2}{ec} \\ k_f = \frac{n_3}{f} \end{cases} \tag{10}$$

where $n1 = n2 = n3 = 6$.

The development of fuzzy control rules has a direct impact on the performance of the controller and usually follows

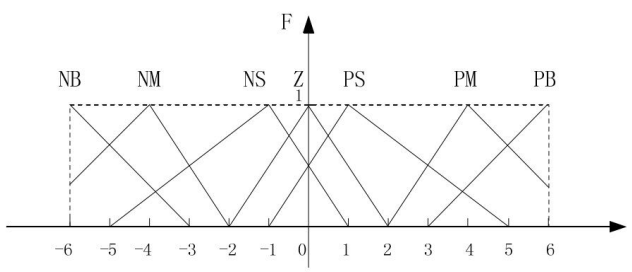

FIGURE 10. Membership function of F

certain rules: when the error is large, the controller should be adjusted in the direction of reducing the error; when the error is small, the controller should avoid overshooting while eliminating the system error to ensure its stability. In the design of the belt conveyor fuzzy controller, the fuzzy control rules can be formulated according to field experience, as shown in Table 1.

TABLE 1. Rules table of fuzzy control

E \F \EC	NB	NM	NS	Z	PS	PM	PB
NB	PB	PB	PB	PB	PM	PS	Z
NM	PB	PB	PB	PM	PS	Z	NS
NS	PB	PB	PM	PS	Z	NS	NM
Z	PB	PM	PS	Z	NS	NM	NB
PS	PM	PS	Z	NS	NM	NB	NB
PM	PS	Z	NS	NM	NB	NB	NB
PB	Z	NS	NM	NB	NB	NB	NB

After the fuzzy rules are established, fuzzy inference is needed to obtain a fuzzy subset of the control quantity. And then the fuzzy inference is completed by converting the fuzzy control quantity into an accurate control quantity using an appropriate method. There are many methods of fuzzy inference, such as median method, centre of gravity method and maximum subordination method.

The fuzzy look-up table is an important part of the fuzzy controller design. When the deviation and the rate of change of the deviation are given, the established fuzzy control look-up table can be used to obtain the corresponding output control quantity. In a belt conveyor control system, the look-up table created off-line can be saved to the PLC memory and obtained by looking up the table when needed, ensuring real-time control.

The query table can be designed with the aid of MATLAB, using the GUI in the Fuzzy Logic Toolbox. The 'Fuzzy Logic Designer' tool is invoked in the MATLAB software to create a two-input, one-output model with input variables E, EC and the output variable P to establish the corresponding. The fuzzy inference output is a three-dimensional surface that represents the relationship between P and E and EC in three-dimensional space. The fuzzy inference output is shown in Figure 11.

Once the fuzzy controller has been designed using the 'MATLAB Fuzzy Toolbox', the fuzzy inference process can be clearly observed using the rule observer, as shown in Figure 12, where the effect of the E and EC subordination functions on the controller output can be observed. When changing the value of the input variables to the observer, the change in the corresponding output can be observed. In Figure 12 , if the input variables $E = -6$ and $EC = -6$ are entered, the corresponding values are entered in the "Input" variable input window and the output $P = 5.37$ is obtained.

In the rule observer, the corresponding variable values are input in the "Input" according to the fuzzy control rule table, and the corresponding output results can be obtained under different inputs, and the final fuzzy control rule table is shown in Table 2 and Table 3.

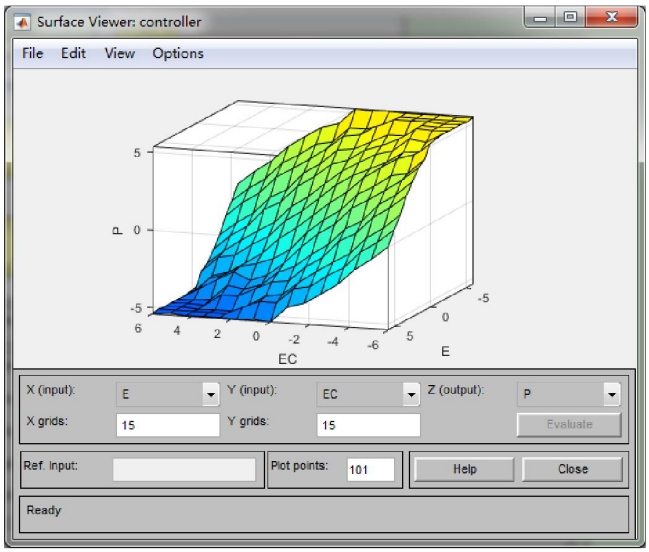

FIGURE 11. Output surface of fuzzy inference

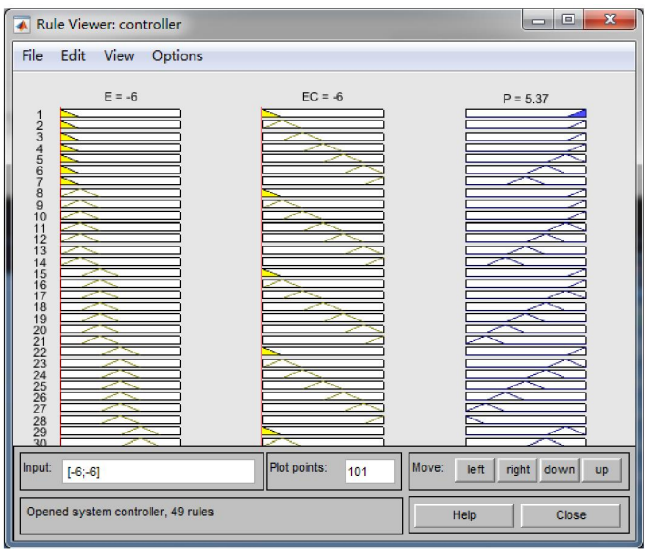

FIGURE 12. Viewer of rule

The belt conveyor fuzzy control system is shown in Figure 13 with a fuzzy controller based on PLC. The belt speed of the electronic belt conveyor is given according to the coal flow information collected by the electronic belt scale. The electronic belt scale is mainly composed of a scale frame, a load cell, a speed sensor and an intelligent acquisition module. The scale frame is the carrier where the load cell and the speed sensor are installed. The load cell converts the weight signal of the material into a power signal, and the speed sensor obtains the speed of the material. Finally, the intelligent acquisition module performs data processing and calculation to obtain the instantaneous flow and Cumulative volume.

Assuming a period of time, the coal flow volume changes in the interval of $[q_0, q_1]$, the corresponding belt given speed

TABLE 2. Query table of fuzzy control

E\F\EC	-6	-5	-4	-3	-2	-1
-6	5.04	4.86	5.04	4.86	5.04	4.86
-5	4.86	4.86	4.86	4.86	4.86	4.27
-4	5.04	4.86	5.04	4.86	5.04	4.27
-3	4.86	4.27	4.27	4.27	4.27	2.77
-2	5.04	4.27	4.21	4.22	4.21	2.72
-1	4.86	4.27	4.22	2.72	2.72	2.22
0	5.04	4.27	4.21	2.72	1.67	1.27
1	4.27	2.77	2.72	2.22	1.27	0
2	4.21	2.72	1.67	1.27	0	-1.27
3	2.72	2.22	1.27	-0.85	-2.26	-2.22
4	1.67	1.27	0	-2.26	-4.21	-4.22
5	1.27	0	-1.27	-2.22	-4.22	-4.27
6	0	-1.27	-1.67	-2.72	-4.21	-4.27

TABLE 3. Query table of fuzzy control

E\F\EC	0	1	2	3	4	5	6
-6	5.04	4.27	4.21	2.72	1.67	1.27	0
-5	4.27	4.27	4.22	2.22	1.27	0	-1.27
-4	4.21	4.22	4.21	2.26	0	-1.27	-1.67
-3	2.72	2.22	2.26	0.85	-1.27	-2.22	2.72
-2	1.67	1.27	0.85	-1.27	-1.67	-2.72	-4.21
-1	1.27	0	-1.27	-2.22	-2.72	-2.77	-4.27
0	0	-1.27	-1.67	-2.72	-4.21	-4.27	-5.04
1	-1.27	-2.22	-2.72	-4.22	-4.22	-4.27	-4.86
2	-1.67	-2.72	-4.21	-4.22	-4.21	-4.27	-5.04
3	-2.72	-2.77	-4.27	-4.27	-4.27	-4.27	-4.86
4	-4.21	-4.27	-5.04	-4.86	-5.04	-4.86	-5.04
5	-4.27	-4.86	-4.86	-4.86	-4.86	-4.86	-4.86

is v_0 and the speed sensor obtains the actual operating speed v of the belt at the same time. The input signal is processed by PLC-based fuzzy controller. Speed deviation (e) and speed deviation change rate (ec) are input into the fuzzy controller based on PLC. After the PLC-based fuzzy controller analysis and calculation, it outputs set frequency signal of inverter. In the PLC-based fuzzy controller, the control signal f is put into the inverter controller, and the frequency and voltage signal of the motor are adjusted through the inverter to realize the control of the operating speed of the belt conveyor.

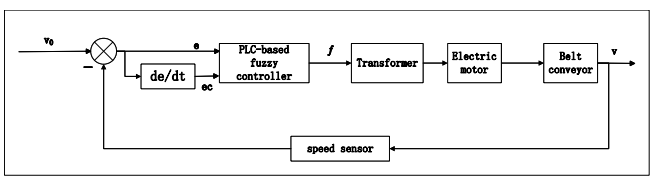

FIGURE 13. Schematic diagram of fuzzy control system for belt conveyor

The fuzzy control query table obtained in the design of the fuzzy controller [19], which gives the frequency setting signal f and the speed deviation e and deviation variable change ec in order to ensure the PLC-based fuzzy control [20] of the velocity deviation e and the velocity deviation rate ec. The real-time reliability of the device is obtained by the vague control of the query table and storing the offline query table in the PLC memory card. When working in the system, the quantification value of the speed deviation and deviation of the PLC sampling is obtained by querying the control table, and then multiplied by the proportional factor to get the frequency value of the inverter, thereby realizing the belt conveyor transportation intelligent control of the machine.

C. BELT CONVEYOR POWER CALCULATION

The total resistance of belt conveyor operation can be divided into four categories: main resistance, inclined resistance, additional resistance and special resistance. Among them, the specific resistance accounts for a very small component, which can often be ignored in the calculation process. Therefore, the circumferential force of the drive pulley of the belt conveyor is:

$$F_{\mathrm{a}} = F_{\mathrm{H}} + F_{it} + F_{\mathrm{v}} = \sum_{i=1}^{n} Cl_i f_i g \left[q_{RO} + q_{RU} + (2q_B + q_G \cos\beta_i\right] + \sum_{i=1}^{n} q_G l_i g \sin\beta_i \tag{11}$$

Generally speaking, the maximum load capacity of the belt conveyor is a definite value at the time of design, which is determined by the belt running speed, the maximum cross-sectional area of the material and the density of the material. The instantaneous flow is related to the running speed of the belt, the specific formula is as follows:

$$q_G = \frac{Q}{3.6v} (v \neq 0) \tag{12}$$

where Q is the instantaneous flow rate of coal transported by the belt, and v is the running speed of the belt.

$$P_A = F_{\mathrm{n}} v \tag{13}$$

The drive roller shaft power can be calculated as:

$$P_A = \sum_{i=1}^{n} Cl_i f_i g\nu \left[q_{RO} + q_{RU} + 2q_B \cos\beta_i\right] + \sum_{i=1}^{n} \frac{Q}{3.6} l_i g \left[Cf_i \cos\beta_i + \sin\beta_i\right] \tag{14}$$

In coal gangue production, the motor and the driving drum are connected through a coupling and a reducer, so there is a certain power loss. For long-distance and high-power belt conveyors, it is often necessary to be equipped with multiple motor drives, and the simultaneous operation of multiple motors will cause power imbalance and power loss. In coal mine production, the relationship between the shaft power of the motor and the shaft power of the drive drum is as follows:

$$P_M = K_1 K_2 P_A \tag{15}$$

where $K_1 = 1/\left(\eta_1 \cdot \eta_2 \cdot \eta_3\right)$, P_M is the motor shaft power, K_1 is the motor power coefficient, K_2 is the motor starting mode coefficient, η_1 is the transmission coefficient of the reduction gear, η_2 is the voltage drop coefficient, and η_3 is

the multi-machine power unbalance coefficient. The motor power can be calculated as:

$$P_M = \sum_{i=1}^{n} K_1 K_2 C l_i f_i g \nu \left[q_{RO} + q_{RU} + 2q_B \cos\beta_i\right] + \sum_{i=1}^{n} \frac{Q}{3.6} K_1 K_2 l_i g \left[C f_i \cos\beta_i + \sin\beta_l\right] \tag{16}$$

When the belt conveyor is in stable operation, its motor power coefficient K, motor starting mode coefficient K_1, resistance coefficient C, section belt length l_j, gravity acceleration g, weight $q_R O$ of the idler roller rotating part of the belt unit length in the up section, The weight $q_R U$ of the rotating part of the belt roller per unit length in the down section, the weight q_B of the belt per unit length, and the inclination angle η_1 of the section belt are all constant values, so the power required to drive the pulley is only related to the material flow Q and the belt running speed v is related to the friction coefficient if of the belt.

For a belt conveyor running stably, the frictional resistance coefficient f_i is constant, and the shaft power P_M of the motor is only related to the material flow Q and the belt running speed v. When the belt running speed v is constant, the material flow Q increases, the coal supply increases, and the motor shaft power P_M increases; and when the material flow is constant, the belt running speed v increases, and the motor shaft power P_M will also increase. And if the running state of the belt conveyor changes, the frictional resistance coefficient f_i will also change. The frictional resistance coefficient f_i of the belt is related to the load, and the belt load is proportional to the material flow Q and inversely proportional to the belt running speed v .

There is a complex relationship between the shaft power P_M of the motor driving the belt and the material flow Q , the belt running speed v and the friction coefficient f_i of the belt, which is difficult to analyze by establishing an accurate mathematical model. In order to better analyze the relationship between the power consumption of the belt conveyor, the running speed of the belt and the flow of the material, it is necessary to collect relevant data on the production site, and use the acquired data to analyze the impact of the running speed of the belt and the flow of the material on the belt. The influence of the power consumption of the conveyor.

VII. EXPERIMENT AND RESULTS ANALYSIS

A. EXPERIMENT PROCEDURE

In order to verify the feasibility of the coal detection method of laser and binocular visual fusion, experimental verification was performed. The obtained dense point cloud data can be visualized and facilitated to directly observe the shape of the coal measurement and the current operating state of the conveyor belt. In order to reduce the impact of the conveyor's own vibration on the measurement results, the average value of the continuous multi-frame conveyor belt empty-loaded cloud data is calculated as the empty load data of the conveyor belt, and the outline of the single-frame coal contour data is directly observed. The contour of the conveyor belt is shown in Figure 14. Selecting a frame of coal contour data is shown in Figure 15.

FIGURE 14. Perform belt empty contour

FIGURE 15. Single-frame coal contour

For three-dimensional reconstruction for the point cloud data for a period of time, the top of the tablet is listed in the ASCII yard format. The two adjacent clouds are generated between the corner lines to generate a triangular face in the form of diagonal. And vertical upward direction is used as a triangular dough line method. The model vertex coordinate corresponding to the point cloud data is set in a real proportion. The point cloud data of the conveyor belt is loaded and the central line of the conveyor belt is used as a model file coordinate axis, and the generated result by STL (Standard Template Library) model is shown in Figure 16.

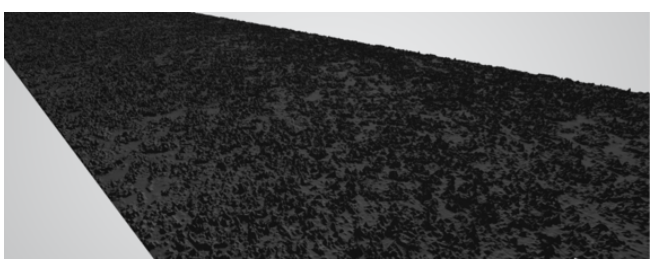

FIGURE 16. Generated STL model

The MATLAB is used to calculate the volume of the coal material in the interval. The total width of the conveyor belt is 80cm and the cross-sectional data of the coal material in Figure 15 is 261.89 cm^2. The volume of the 2 meters coal volume is 54734.72 cm^3. Checking the information and knowing that the volume density of lignite is 1.1 g/cm^3. It can be seen that the amount of coal transported 2 meters transported by the conveyor belt is 60208.192 g, which is about 60 kg of coal.

The energy-saving optimization model established by the BP neural network is used to build a non-linear relationship

of the conveyor coal flow volume (Q), the belt conveyor speed (v) and the power (P) of the belt. When Q is determined by the coal flow of the belt, the power-saving optimization model can be obtained by the constructed energy-saving optimization model. Set $q = 500t/h$, and the belt is running at $1.70m/s < 4.40m/s$. When the energy-saving optimization model predicts $Q = 500t/h$, v is in the interval $[1.74, 4.38]$. It can be found that the minimum value in this interval is $957.06kW$, and the corresponding belt operating speed is $v = 2.00m/s$. Using this method, you can obtain the corresponding optimal solution v under different coal flows. In actual transportation, coal flow is constantly changing. If the controller design is too sensitive, frequent deceleration control will increase the system power loss. Therefore, the Q can use $25t/h$ as an incremental statistics, and to obtain the optimal solution of the system under different coal flow through the energy-saving optimization model built. Specifically, as shown in Table 4, the Q change range of Q is $[0, 1100]$, and the v changing range is $[1.74, 4.40]$. The controller can be designed according to the optimization list of the operating speed of the belt.

In actual transportation, the coal flow rate is constantly changing. If the controller design is too sensitive, frequent acceleration and deceleration control will increase the power loss of the system. Therefore, the coal flow Q can be counted in increments of $25t/h$, and the optimal solution of the system under different coal flow conditions can be obtained through the constructed energy-saving optimization model, as shown in Table 4, where the change interval of Q is $[0, 1100]$, and the variation range of v is $[1.74, 4.40]$. According to the established belt running speed optimization list, the controller can be designed.

TABLE 4. Optimization table of belt running speed

Q/(t/h)	v (m/s)	P(KW)	Q/(t/h)	v (m/s)	P(KW)	Q/(t/h)	v (m/s)	P(KW)
0	1.74	147.89	375	1.74	755.25	750	2.98	1363.49
25	1.74	183.10	400	1.75	795.84	775	3.08	1399.81
50	1.74	219.83	425	1.76	829.92	800	3.20	1445.48
75	1.74	262.73	450	1.79	876.58	825	3.29	1490.00
100	1.74	306.08	475	1.88	913.16	850	3.40	1526.47
125	1.74	347.71	500	2.00	957.06	875	3.48	1565.12
150	1.74	387.19	525	2.08	994.01	900	3.59	1607.82
175	1.74	423.83	550	2.19	1034.87	925	3.69	1645.51
200	1.74	471.09	575	2.29	1075.73	950	3.78	1688.58
225	1.74	509.19	600	2.40	1118.44	975	3.88	1734.32
250	1.74	554.49	625	2.49	1159.24	1000	3.97	1775.69
275	1.74	593.09	650	2.58	1203.47	1025	4.07	1812.99
300	1.74	631.73	675	2.69	1239.01	1050	4.18	1849.06
325	1.74	667.15	700	2.79	1286.91	1075	4.28	1891.11
350	1.74	711.04	725	2.89	1324.23	1100	4.38	1940.94

It can be seen from Table 4 that when Q in the interval $[0, 400]$, the operating speed of the belt is $1.74m/s$, and the power of the belt conveyor increases with the increase of the coal flow; The operating speed of the belt and the power of the belt conveyor increased with the increase in coal flow.

In coal mine production, the coal flow of the belt conveyor is uneven. In order to improve the stability of the control system, the coal flow information at a certain moment can use the average value of the coal flow within 10 seconds before the moment as a reference value. In order to realize the energy-saving operation of the belt conveyor, the running speed of the belt should be matched with the coal flow. At the same time, in order to avoid the disturbance caused by the coal flow, the coal flow can be divided into multiple intervals. According to the relationship between belt running speed and coal flow established in Table 4, the reference coal flow value $12.5t/h$ is taken as an interval. When the measured value of coal flow fluctuates in this interval, the reference value of coal flow can be considered to be basically unchanged.

B. DISCUSSION

The experimental results prove that this plan has good real-time nature and can complete the detection task of coal volume well. By analyzing the experimental process, the main reasons for the summary volume calculation error are:

- There is still an error in the calculation process of the camera calibration and the three-dimensional matching calculation.
- The running state is not fixed and there is an error in using the average method of continuous multi-frame air load.
- Observation of laser wiring and binocular cameras from top to bottom and there is no way to detect air gap between coal blocks, which causes errors.
- The number of binocular camera frames is fixed and the speed change of the conveyor belt will also change the information integrity between the neighboring clouds.

We took the coal mine belt conveyor as the research object and designed the belt conveyor intelligent control system for energy-saving operation. Our methods optimized the control of belt running speed to achieve the expected effect. However, there are inevitable shortcomings in the paper:

- When collecting data samples, due to the influence of coal mine production, the acquired data samples are not large enough, which affects the accuracy of the final energy-saving model.
- In addition, due to the limited time, this paper only analyzed the energy-saving problem of single belt conveyors and did not provide a solution for the joint energy-saving control of multiple belt conveyors.

VIII. CONCLUSION

A merging laser scanning and binocular visual coal flow detection method is proposed. Both the non-contact detection methods are fused, which can greatly reduce the impact of measurement accuracy in coal mines and the harsh environment. The binocular visual camera calibration system was studied and the image filtering and cutting were preprocessed using image filtering and cutting, reducing the actual computing amount and improving the real-time nature of the system. The semi-global matching algorithm is used to obtain the coal contour point cloud data and the depth data when the conveyor belt is air-loading. Based on the differences between the two data, two-dimensional and three-dimensional visualization of point clouds are performed. The

cross-section area between the same cross-section adjacent point uses a trapezoidal cumulative method and combines the frame rate of the camera, the current speed, and coal accumulation density, it can be calculated for a period of time for the conveyor belt coal volume. And then we applied the BP neural network to establish an energy-saving optimization model for coal flow volume, belt operation speed, and system power consumption. The energy-saving optimization model obtains the optimal speed value of the belt conveyor with different coal flow volumes; Based on the introduction of fuzzy control algorithms, the design of the PLC fuzzy controller is completed and the operating speed of the belt can be intelligently adjusted according to the size of the coal flow volume. Finally, the energy-saving operation and intelligent control of the belt conveyor can be achieved.

REFERENCES

[1] S. W. Wang and L. I. Chuan-Jiang, "Design of electronic belt scale instrument based on arm," *Machinery Electronics*, 2013.
[2] N. Mihuţ, "Designing a system for measuring the flow of material transported on belts using ultrasonic sensors," in *IOP Conference Series: Materials Science and Engineering*, vol. 95, no. 1. IOP Publishing, 2015, p. 012089.
[3] C. Noss, J. Wilkinson, and A. Lorke, "Triangulation hand-held laser-scanning (trihalas) for micro-and meso-habitat surveys in streams," *Earth Surface Processes and Landforms*, vol. 43, no. 6, pp. 1241–1251, 2018.
[4] X. C. Dong, "Research on implementation method of basic components of neural network for belt weigher by fpga," 2019.
[5] L. Xianguo, S. Lifang, M. Zixu, Z. Can, and J. Hangqi, "Laser-based online machine vision detection for longitudinal rip of conveyor belt," *Optik*, vol. 168, pp. 360–369, 2018.
[6] Y. Wang, W. Guo, S. Zhao, B. Xue, and Z. Xing, "A scraper conveyor coal flow monitoring method based on speckle structured light data," *Applied Sciences*, vol. 12, no. 14, p. 6955, 2022.
[7] G. Wang, X. Li, and L. Yang, "Dynamic coal quantity detection and classification of permanent magnet direct drive belt conveyor based on machine vision and deep learning," *International Journal of Pattern Recognition and Artificial Intelligence*, vol. 35, no. 11, p. 2152017, 2021.
[8] Y. Lv, B. Liu, N. Liu, and M. Zhao, "Design of automatic speed control system of belt conveyor based on image recognition," in *2020 3rd International Conference on Artificial Intelligence and Big Data (ICAIBD)*. IEEE, 2020, pp. 227–230.
[9] J. Hiltermann, G. Lodewijks, D. Schott, J. Rijsenbrij, J. Dekkers, and Y. Pang, "A methodology to predict power savings of troughed belt conveyors by speed control," *Particulate science and technology*, vol. 29, no. 1, pp. 14–27, 2011.
[10] S. Zhang and X. Xia, "Modeling and energy efficiency optimization of belt conveyors," *Applied energy*, vol. 88, no. 9, pp. 3061–3071, 2011.
[11] J. Ji, C. Miao, and X. Li, "Research on the energy-saving control strategy of a belt conveyor with variable belt speed based on the material flow rate," *Plos one*, vol. 15, no. 1, p. e0227992, 2020.
[12] L. Hao, X. Yang, H. Wang, Y. Wang, and S. U. Jinshan, "Real-time 3d point cloud imaging technology for long-distance target based on binocular stereo vision," *Laser Journal*, 2019.
[13] G. Wu, J. Yang, and H. Yang, "Real-time low-power binocular stereo vision based on fpga," *Journal of Real-Time Image Processing*, no. 1, p. 19, 2022.
[14] Z. Zhang, "Flexible camera calibration by viewing a plane from unknown orientations," in *Proceedings of the seventh ieee international conference on computer vision*, vol. 1. Ieee, 1999, pp. 666–673.
[15] C. Yu, F. Ji, and J. Xue, "Dynamic granularity matrix space model based high robust multi-ellipse center extraction method for camera calibration," *IEEE Access*, vol. 8, pp. 128 308–128 323, 2020.
[16] X. Xu, Z. Fei, J. Yang, Z. Tan, and M. Luo, "Line structured light calibration method and centerline extraction: A review," *Results in Physics*, vol. 19, p. 103637, 2020.
[17] J. Li, J. Zhang, H. Wang, and B. Feng, "Coal flow volume measurement of belt conveyor based on binocular vision and line structured light," in *2021 IEEE International Conference on Electrical Engineering and Mechatronics Technology (ICEEMT)*. IEEE, 2021, pp. 636–639.
[18] C. Zhou, H. Yu, B. Yuan, L. Wang, and Q. Yang, "Three-dimensional stitching of binocular endoscopic images based on feature points," *Multidisciplinary Digital Publishing Institute*, no. 8, 2021.
[19] J. Zhao, L. I. Duan-Neng, and C. Wang, "Pid fuzzy controller and measurement research of magnetic navigation agv based on mitsubishi plc," *Measurement Control Technology*, 2019.
[20] A. Gizi, "Plc fuzzy pid controller of mppt of solar energy converter," *WSEAS Transactions on Systems and Control*, vol. 16, pp. 1–20, 2021.

LIANG WEN graduated with a master's degree and is currently the deputy general manager of CCTEG China Coal Research Institute; member of the 5th Coal Industry Coal Mine Safety Standardization Technical Committee Gas Detection and Rescue Equipment Branch, Member of the 4th Coal Industry Technical Committee Coal Mine Intelligence and New Technology Expert Committee, member of the 1st Young Expert Committee of "Industry and Mining Automation" magazine, and external tutor of the postgraduate school of Liaoning Technology University. He has presided over and completed 2 major national science and technology projects, 2 national science and technology support plan projects, 1 national international cooperation project, He has won 15 awards above the provincial and ministerial level, including 2 national patent awards for excellence, 5 first prizes, 4 second prizes and 5 third prizes. He has published more than 20 academic papers in core academic journals, 18 authorized patents (including 11 invention patents) and 22 software copyrights. He has won the Sun Yueqi Youth Science and Technology Award, the National Coal Youth May 4th Medal, and the China Coal Industry Association Advanced Individual in the Integration of Industrialization and Industrialization.

BING LIANG was born in December 1962, from Dawa, Liaoning. Member of the Communist Party of China, Ph.D., professor and doctoral supervisor of the Mining Department of Northeastern University. She successively served as the deputy director and director of the Research Office of Liaoning Technology University, the dean of the Graduate School, the vice president of Liaoning Technology University, the deputy secretary of the Party Committee and the president of Liaoning Technology University. She is the Secretary of the Party Committee of Liaoning Technology University, currently.

LIYA ZHANG (Member, IEEE) received the M.S. degree from the China University of Mining and Technology, Beijing, in 2012. He is currently pursuing the Ph.D. degree at the School of Electronic and Information Engineering, Beijing Jiaotong University. He works as the Chief Expert (second-level) of CCTEG China Coal Research Institute, and the Director of the Smart Mining Institute. His current research interests include coal mine 5G communication, coal mine safety monitoring systems, and emergency rescue communication.

BONAN HAO was born in Tangshan, Hebei, China in 1993. He graduated from the China University of Mining and Technology (Beijing) in 2019 with a master's degree. Now he is working in CCTEG China Coal Research Institute, as a research assistant. He has been engaged in the research of mine artificial intelligence, including research and technology development in mining machine vision, big data, deep learning, and other fields.

ZHIFANG YANG was born in Luoyang, Henan, China in 1994. He obtained a master's degree in the School of Automation, University of Science and Technology Beijing, China, in 2022. Now, He is working at CCTEG China Coal Research Institute, studying in the fields of control science and engineering, deep learning, mine, and industrial intelligence. He has published two EI conference as the first author, and participated in the publication of four SCI papers.